Combined Effects of Deforestation and Doubled Atmospheric CO$_2$ Concentrations on the Climate of Amazonia

Marcos Heil Costa* and Jonathan A. Foley

Climate, People and Environment Program, Institute for Environmental Studies, and Department of Atmospheric and Oceanic Sciences, University of Wisconsin—Madison, Madison, Wisconsin

ABSTRACT

It is generally expected that the Amazon basin will experience at least two major environmental changes during the next few decades and centuries: 1) increasing areas of forest will be converted to pasture and cropland, and 2) concentrations of atmospheric CO$_2$ will continue to rise. In this study, the authors use the National Center for Atmospheric Research GENESIS atmospheric general circulation model, coupled to the Integrated Biosphere Simulator, to determine the combined effects of large-scale deforestation and increased CO$_2$ concentrations (including both physiological and radiative effects) on Amazonian climate.

In these simulations, deforestation decreases basin-average precipitation by 0.73 mm day^{-1} over the basin, as a consequence of the general reduction in vertical motion above the deforested area (although there are some small regions with increased vertical motion). The overall effect of doubled CO$_2$ concentrations in Amazonia is an increase in basin-average precipitation of 0.28 mm day^{-1}. The combined effect of deforestation and doubled CO$_2$, including the interactions among the processes, is a decrease in the basin-average precipitation of 0.42 mm day^{-1}. While the effects of deforestation and increasing CO$_2$ concentrations on precipitation tend to counteract one another, both processes work to warm the Amazon basin. The effect of deforestation and increasing CO$_2$ concentrations both tend to increase surface temperature, mainly because of decreases in evapotranspiration and the radiative effect of CO$_2$. The combined effect of deforestation and doubled CO$_2$, including the interactions among the processes, increases the basin-average temperature by roughly 3.5°C.

1. Introduction

Deforestation in Amazonia has been occurring since European settlers arrived in Brazil; however, the intensity of deforestation has increased dramatically in the last few decades. Using remote sensing imagery, Fearnside (1993) estimated that, by 1991, 426 000 km^2 of the Amazon forest had already been removed (10.5% of the original forest area of 4×10^6 km^2). Between 1978 and 1988, deforestation occurred at an average rate of 22 000 km^2 yr^{-1}, varying between 11 000 and 29 000 km^2 yr^{-1} since then (Fearnside 1993; Krug 1998; Fig. 1a). The highest deforestation rates, which occurred in the late 1970s and early 1980s, were a consequence of the intensive migration of people into Amazonia (Page 1995).

Numerous studies have used atmospheric general circulation models (AGCMs) to examine the possible effects of Amazonian deforestation on global and regional climates (Table 1). While it is difficult to give a comprehensive overview of all of the AGCM Amazonian deforestation simulations performed to date, a few general results have emerged from these simulations. All of the AGCM deforestation simulations show a significant increase in temperature, and a significant decrease in evapotranspiration over the basin after deforestation. In addition, most (but not all) of the deforestation simulations show a significant decrease in precipitation over the Amazon basin in response to deforestation. However, these simulations totally disagree on the magnitude (and even the sign) of runoff changes after deforestation. Runoff is one of the most uncertain results of these models, as it arises from the difference between two relatively large quantities (precipitation and evapotranspiration).

Other important climatic factors may also change during the time frame of the anticipated deforestation. In particular, atmospheric CO$_2$ concentrations may continue to rise during the next two centuries. For example, Fig. 1b shows projections of Amazonian deforestation (extrapolating the average 1978–96 rate forward in time) and atmospheric CO$_2$ concentrations (using sce-

---

* Additional affiliation: Departamento de Engenharia Agrícola, Universidade Federal de Viçosa, Vicosa, Brazil.

Corresponding author address: Dr. Jonathan A. Foley, Center for Climate Research, University of Wisconsin—Madison, 1225 West Dayton Street, Madison, WI 53706-1695.
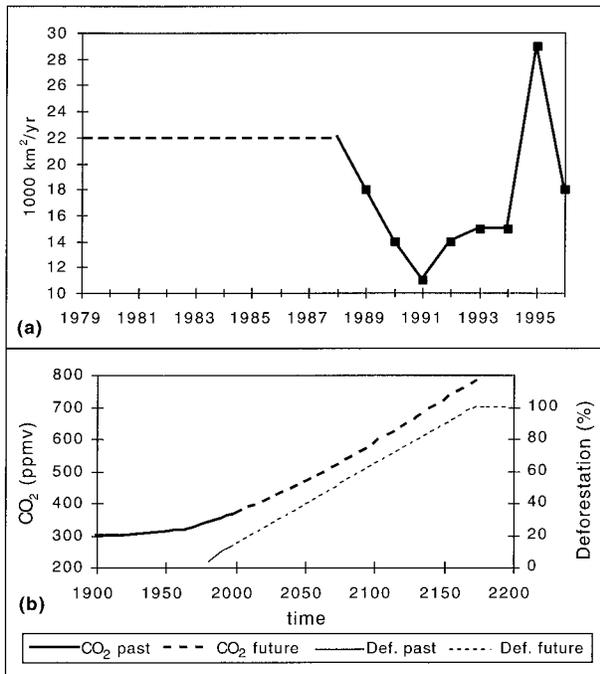E-mail: jfoley@facstaff.wisc.edu

FIG. 1. (a) Historic rates of Amazonian deforestation (Fearnside 1993; Krug 1998), (b) scenarios of Amazonian deforestation and scenarios of atmospheric CO_2 (Houghton et al. 1990).

nario B of the 1990 Intergovernmental Panel on Climate Change report until 2100 and an extrapolation using the same growth rate thereafter). According to these scenarios, when the CO_2 levels reach twice their present level, Amazonian deforestation will be nearly complete. Of course, these simple scenarios should not be treated as any kind of prediction of future environmental conditions; they are simply extrapolations of current trends. Undoubtedly, these current trends will change over time, in response to changing population and economic pressures. Nevertheless, it seems likely that, in the future, Amazonia will experience an increasing area of deforested lands and higher CO_2 concentrations.

The natural question arises, What would be the *combined* effects of increased atmospheric CO_2 concentrations *and* deforestation on the climate of the Amazon basin? This study makes use of a series of climate model simulations with the GENESIS (version 2) AGCM to analyze the response of Amazonian climate to deforestation, a doubling of atmospheric CO_2 concentrations, and a combination of the two effects.

2. CO_2 and Amazonian climate: Radiative and physiological effects

There are at least two entirely different potential effects of CO_2 concentrations on the earth's climate system. The most widely discussed is the radiative effect of CO_2 molecules in the atmosphere as a greenhouse gas, with the consequent changes in the atmospheric

TABLE 1. Comparison of some recent AGCM Amazonian deforestation experiments designs and results.

Reference	Dickinson and Kennedy (1992)	Henderson-Sellers et al. (1993)	Lean and Rowntree (1993)	Polcher and Laval (1999)	Sud et al. (1996)	Manzi and Planton (1996)	Lean and Rowntree (1997)	Hahmann and Dickinson (1997)	This study (D)
AGCM	CCM1	CCM1-OZ	UKMO	LMD	GLA	EMERAUDE	UKMO	RCCM2	GENESIS
Resolution	4.5° × 7.5°	4.5° × 7.5°	2.5° × 3.75°	2.0° × 5.6°	4.0° × 5.0°	2.8° × 2.8°	2.5° × 3.75°	2.8° × 2.8°	4.5° × 7.5°
Surface model	BATS (Dickinson et al. 1986)	BATS (Dickinson et al. 1986)	Warrilow (Warrilow et al. 1986)	SECHIBA (Ducroudé et al. 1993)	SSiB (Xue et al. 1991)	ISBA (Noilhan and Planton 1989)	Warrilow (Warrilow et al. 1986) Modified	BATS 1e (Dickinson et al. 1993)	IBIS (Foley et al. 1996)
Ocean	Mixed layer	Mixed layer	Prescribed SST	Prescribed SST	Prescribed SST	Prescribed SST	Prescribed SST	Mixed layer	Mixed layer
Simulation length	3 yr	6 yr	3 yr	1.1 yr	3 yr	3 yr	10 yr	10 yr	15 yr
Roughness (m)	2.00/0.05	2.00/0.20	0.80/0.04	2.30/0.06	2.65/0.077	2.00/0.026	2.10/0.026	2.00/0.05	**1.51/0.05**
Albedo	0.12/0.19	0.12/0.19	0.14/0.19	0.098/0.177	0.092/0.142	0.12/0.163	0.13/0.18	0.12/0.19	**0.135/0.173**
ΔP (mm day^{-1})	−1.4	−1.6	−0.8	+1.1	−1.5	−0.4	−0.4	−1.0	**−0.7**
ΔE (mm day^{-1})	−0.7	−0.6	−0.6	−2.7	−1.2	−0.3	−0.8	−0.4	**−0.6**
ΔR (mm day^{-1})	−0.7	−0.9	−0.2	+3.8	−0.3	+0.3	+0.4	−0.6	**−0.1**
ΔT (mm day^{-1})	+0.6	+0.6	+2.1	+3.8	+2.0	+1.3	+2.3	+1.0	+1.4

energy balance and temperature climate (see Mitchell et al. 1990; Kattenberg et al. 1996). In addition, there is a separate effect of atmospheric CO_2 on climate through the dependence of vegetation canopy processes on CO_2 concentration; a higher partial pressure of CO_2 in the atmosphere often stimulates canopy photosynthesis and decreases stomatal conductance. The result of these physiological effects may lead to an overall decrease in canopy transpiration, hence affecting the water and energy balance of the land surface.

Only a few modeling studies have examined the physiological effects of CO_2 on land surface processes and climate. Pioneering studies exploring the physiological effects of CO_2 on land surface processes and climate were performed by Pollard and Thompson (1995) and Henderson-Sellers et al. (1995). However, in these two studies, the physiological effects of doubled CO_2 were assumed to result in a halving of stomatal conductance, which may be an exaggeration. A more realistic simulation was conducted by Sellers et al. (1996a), wherein they coupled an AGCM to the physiologically based SiB2 land surface model. Sellers et al. did not present results for the Amazon basin specifically, but for the Tropics they reported that a doubling of CO_2 caused canopy conductance to decrease by 26% and annual mean evapotranspiration to decrease by 4%. Furthermore, Sellers et al. compared the response of the climate system to the combination of radiative and physiological CO_2 effects. Over the tropical land masses, they report changes in evapotranspiration (-4.1, $+5.1$, and $+1.8$ W m^{-2}), precipitation (-0.02, $+0.22$, $+0.22$ mm day^{-1}), and temperature ($+0.4$, $+1.7$, $+2.1°$C) in response to physiological effects, radiative effects, and the combination of the two, respectively.

At least one study has specifically focused on the response of Amazonian ecosystems to the physiological effects of doubled CO_2 concentrations. Costa and Foley (1997) used the LSX land surface model of Pollard and Thompson (1995) (modified to include physiologically based formulations of photosynthesis and canopy conductance) with prescribed climate forcing. They reported that a doubling of atmospheric CO_2 concentrations decreased the average canopy conductance of the rainforest and grassland regions by 34% and 32%, respectively. In addition, they found that annual mean evapotranspiration decreased by 4.5% and 2.8% in rainforest and grassland regions, respectively.

However, the work of Costa and Foley (1997) neglects the potential importance of humidity feedbacks on transpiration within the planetary boundary layer (Jarvis and McNaughton 1986; Monteith 1995) and changes in the climate that feed back on the hydrologic cycle. In order to address fully the potential sensitivity of freshwater resources to changes in CO_2 concentration, this study uses an AGCM to consider the complex relationships among atmospheric, biophysical, and hydrological processes. Furthermore, these processes are examined against a backdrop of potential changes in land cover resulting from extensive deforestation.

3. Model description

This study is performed using the GENESIS AGCM version 2. Thompson and Pollard 1995a,b; Pollard and Thompson 1995). We employed the model at a R15 horizontal resolution (approximately 4.5° lat $\times$ 7.5° long), with 16 levels in a hybrid sigma pressure vertical coordinate system (sigma near the ground, pressure at the top of the atmosphere). GENESIS also includes an ocean model, in the form of a 50-m slab mixed layer ocean model with sea ice.

We use R15 resolution in this study mainly for computational efficiency. However, R15 resolution is sometimes considered too coarse for some AGCM applications, as it may not be able to resolve some important features of regional climates. On the other hand, using high-resolution AGCMs does not always guarantee better results. For example, a state-of-the-art modeling study [using the National Center for Atmospheric Research (NCAR) CCM3 at T42 resolution, or 2.8° $\times$ 2.8°] of Amazonian climate by Hahmann and Dickinson (1997) simulated $\sim$10 mm day^{-1} precipitation in northeast Brazil where the climatology is $\sim$6 mm day^{-1}. In addition, Costa and Foley (1998) evaluated the precipitation simulation from the high resolution National Centers for Environmental Prediction–NCAR model reanalysis dataset, finding serious biases in the simulated precipitation even at this very high spatial resolution. A more important factor may be the AGCM cloud parameterization (Manzi and Planton 1996; cf. the experiments of Polcher and Laval 1994a,b).

This version of GENESIS has been coupled to the Integrated Biosphere Simulator (IBIS) biosphere model (Foley et al. 1996) to calculate the exchanges between the land surface and the atmosphere. IBIS is built on the original GENESIS land surface model (LSX; Pollard and Thompson 1995), with the addition of canopy physiological functions, terrestrial carbon cycling, and vegetation dynamics. Further discussion of the biosphere model was provided by Pollard and Thompson (1995) and Foley et al. (1996).

Like the LSX land surface model, IBIS represents the temperature of the soil and the vegetation canopies, as well as the temperature and specific humidity within the canopy air spaces. Changes in temperature and humidity are forced by the radiation balance of the canopies and the soil surface, as well as the diffusive and turbulent fluxes of water vapor and sensible heat. The transfer of solar radiation within each vegetation layer is described using a two-stream approximation, with independent calculations for direct and diffuse radiation in two wave bands (0.3–0.9 and 0.9–4.0 μm). Longwave radiation is simulated as if each vegetation layer is a semitransparent plane with a foliage-dependent emissivity. The effective albedo of the vegetation is calculated rather

than prescribed and depends on the amount of leaf area (LAI) and the orientation and reflectance of leaves. Wind speeds are modeled using a logarithmic profile outside the vegetation canopies and using a simple diffusive parameterization within each vegetation layer. The roughness lengths of each vegetation layer are also computed during the process. A six-layer soil model (layers of 0.10-, 0.15-, 0.25-, 0.50-, 1.00-, and 10.00-m thickness, respectively) is used to capture the diurnal, seasonal and interannual variations in soil temperature, soil moisture, and soil ice. With this formulation, IBIS is able to simulate surface runoff and deep drainage (which are collectively referred as runoff in this paper).

IBIS simulates stomatal conductance as a function of the photosynthesis rate, the carbon dioxide concentration in the leaf boundary layer, and atmospheric humidity, following the formulation of Leuning (1995). Photosynthesis is simulated using the widely used Farquhar equations (Farquhar et al. 1980; Farquhar and Sharkey 1982), where the rate of photosynthesis is a function of absorbed light, leaf temperature, internal carbon dioxide concentration, and the Rubisco enzyme capacity for photosynthesis. The equations for photosynthesis and stomatal conductance are closed by considering the diffusion of CO_2 through the canopy boundary layer and the leaf (Collatz et al. 1991, 1992). These formulations provide a robust and mechanistic description of canopy physiology and how physiological processes respond to the environment.

IBIS is also capable of simulating changes in vegetation cover, on both seasonal and long-term timescales. On the seasonal timescale, the model simulates the phenology (including leaf drop and regrowth) of leaves of the seasonal vegetation. In this simulation, however, the long-timescale vegetation dynamics (which includes vegetation growth and competition among plant types) is turned off.

4. Experiment design

The following set of simulations is designed to elucidate the combined effects of deforestation and the physiological and radiative effects of CO_2. All of the simulations were run for 15 yr, using the same initial conditions; the last 10 yr are averaged to analyze the results. The first 5 yr are left for the model to approach an equilibrium state, specifically with respect to soil moisture and ocean temperatures.

In this study, we conduct 4 simulations.

1) *F,* the control experiment: Rainforest cover as in Fig. 2; atmospheric concentrations of CO_2 are set to 345 ppmv (1×).
2) *D,* the deforested experiment: All the rainforest covered grid cells in *F* are replaced by grasses; atmospheric concentration of CO_2 is set to 345 ppmv (1×).
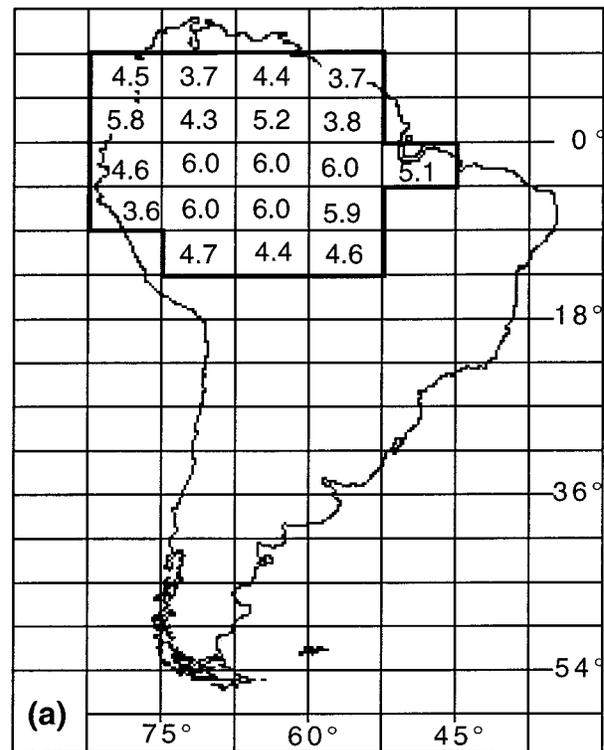3) FPR, the 2 × CO_2 experiment: Vegetation cover as

FIG. 2. Model grid for South America; the grid cells inside the polygon have rainforest in the *F* experiments and pasture in the *D* experiments. The numbers represent the leaf area index of the tropical rainforest.

in *F*; atmospheric concentration of CO_2 is set to 690 ppmv (2×), including both physiological (*P*) and radiative (*R*) effects.
4) DPR, the 2 × CO_2 and deforested experiment: Vegetation cover as in *D*; atmospheric concentration of CO_2 is set to 690 ppmv (2×), for both physiological (*P*) and radiative (*R*) effects.

In order to isolate the physiological effects of CO_2 on the Amazonian climate, we conduct two additional simulations.

5) FP: Vegetation cover as in *F*; atmospheric concentration of CO_2 is set to 690 ppmv (2×), only considering physiological effects (*P*) (the radiative forcing of CO_2 is the same as in the 1 × CO_2 case).
6) DP: Vegetation cover as in *D*; atmospheric concentration of CO_2 is set to 690 ppmv (2×), only considering physiological effects (*P*) (the radiative forcing of CO_2 is the same as in the 1 × CO_2 case).

In Table 1, we compare the simulations performed here with the most recent deforestation experiments conducted by other authors. The major differences between our work and the others include the interactive calculations of albedo and roughness length, the physiologically based calculations of stomatal conductance, and the interactive seasonal phenology of the vegetation

TABLE 2. Vegetation and soil input data used in the *F* and *D* families of experiments.

Parameter	*F* family (F, FP, FPR)	*D* family (D, DP, DPR)
Maximum root depth	12 m	12 m
Percent of roots between 0 and 2 m	87	99
Percent of roots between 2 and 12 m	13	<1
Albedo	interactive	interactive
Roughness length	interactive	interactive
Stomatal conductance	interactive	interactive
Maximum LAI	4.6–6.0	2.7
Reflectance in the 0.3–0.9-μm band	0.19	0.25
Reflectance in the 0.9–4.0-μm band	0.44	0.58
Orientation of leaves	spherical	half spherical, half upright

TABLE 3. Annual-mean results for the control simulation for the rainforest area, and comparisons with other studies. Here, *P* is precipitation, *E* is evapotranspiration, Tr is transpiration, *T* is temperature, LAI is leaf area index, α is albedo, and z_0 is roughness length.

	Simulated (F)	Other studies	Source/notes
P (mm day^{-1})	5.92	6.24	Legates and Willmott (1990)
E (mm day^{-1})	3.86	3.1	Lesack (1993); water balance; catchment
		3.6	Shuttleworth (1988); Manaus
		3.7–4.0	Rocha et al. (1996); simulation
		4.2	Costa and Foley (1997); simulation
		4.1–4.6	Leopoldo (1982)
E/P (%)	65	39	Lesack (1993); water balance; catchment
		65	Costa and Foley (1997); simulation
		65–74	Franken and Leopoldo (1984)
Tr (mm/day^{-1})	2.82	3.14	Costa and Foley (1997)
Tr/E (%)	73	75	Costa and Foley (1997)
T (°C)	25.6	24.8	Culf et al. (1996); Ji-Paraná
		25.7	Culf et al. (1996); Manaus
		25.7	Culf et al. (1996); Marabá
LAI	5.32	4.63	Roberts et al. (1996); Ji-Paraná
		5.38	Roberts et al. (1996); Marabá
		5.7	McWilliam et al. (1993); Manaus
		6.1	Roberts et al. (1996); Manaus
α (%)	13.5	13.2	Culf et al. (1996); average of three sites
z_0 (m)	1.51	2.35	Wright et al. (1996)

cover. In addition, our simulations are somewhat longer than many of the others, which increases the statistical significance of the results and allows enough time for the simulated climate to more closely approach an equilibrium state.

Table 2 summarizes the vegetation and soil boundary conditions used in the *F* and *D* families of experiments. In the *D* group of experiments, the tropical rainforest is replaced by grasses. However, soil characteristics are held constant for all of the experiments. In this study, we use a total soil depth of 12 m to account for the recent findings about deep water extraction by roots in Amazonia (Nepstad et al. 1994; Hodnett et al. 1996). The use of such deep soils required a longer period for the model to reach equilibrium (5 yr). The maximum LAI of the rainforest is shown in Fig. 2, which is generally consistent with the measured values reported by Roberts et al. (1996). In the seasonal forest and in the pasture, the simulated LAI varies during the year according to the soil moisture, without going above the maximum LAI. In the deforested experiment, the pasture was assigned a maximum LAI of 2.7 (Wright et al. 1996) throughout the basin. The reflectance of the leaves is calculated by weighting the reflectance values suggested by Sellers et al. (1996b) to the wave bands 0.3–0.9 and 0.9–4.0 μm, used by the radiation code of GENESIS.

5. Control simulation

In this section, the results of the control simulation are compared to observations from the Amazon Rainforest Micrometeorological Experiment (ARME) (Shuttleworth 1988) and Anglo Brazilian Amazonian Climate Observation Study (ABRACOS) (Gash et al. 1996) experiments, among others. In the following sections, regional averages are calculated considering the region covered by rainforest or pasture, according to Fig. 2.

First, we present a summary of the annual mean simulated climate over the Amazon basin (Table 3). Precipitation appears to be somewhat underestimated compared to the climatological data of Legates and Willmott (1990). The simulated evapotranspiration is within the range of several published estimates, especially with respect to Rocha et al. (1996), which is probably the best available estimate of evapotranspiration in the Amazon rainforest. The ratios of evapotranspiration to precipitation (*E/P*) and transpiration to evapotranspiration (Tr/*E*) are in good agreement with our previous estimates made with the off-line version of IBIS (Costa and Foley 1997). The simulated albedo (α) matches the average albedos in the three sites reported by Culf et al. (1996), while the surface roughness length (z_0) differs from the estimated value by 36% (0.84 m).

Figure 3a presents the seasonal cycle of precipitation, averaged over the forested area, compared with the climatology of Legates and Willmott (1990). The seasonality of evapotranspiration (Fig. 3b) compares very well with the ARME estimates made by Shuttleworth (1988) in Manaus.

A comparison of the simulated spatial patterns of precipitation for the three rainiest (January–March: JFM) and driest (July–September: JAS) months with the climatology of Legates and Willmott (1990) is presented in Fig. 4. Simulated precipitation patterns at R15 are very limited, including the results of this simulation. The simulated patterns for JFM generally agree with the
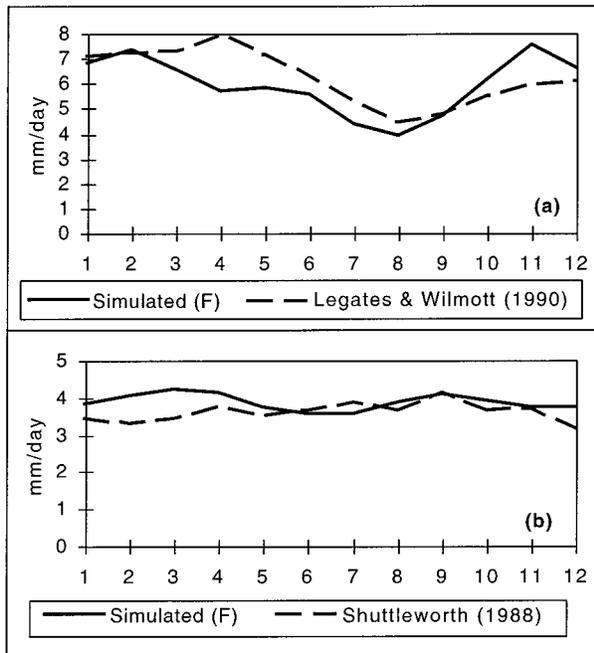
FIG. 3. Seasonal variation of simulated and observed (a) *P* and (b) *E*.

observed, with the exception of a precipitation maximum in northeast Brazil, which is outside the rainforest area. Results look reasonable for northern Amazonia in JAS, but southern Amazonia is drier than observed during this period.

Due to the nature of this study, it was not possible to prescribe the sea surface temperatures (SSTs). Instead, a simple mixed layer ocean model is used, but because it does not represent the ocean circulation, some features of the SST pattern are in error. As a conse-

quence, the SST on the coast of northeast Brazil in JFM is very high (not shown), which probably caused the high convection and high precipitation (Fig. 4a) in northeast Brazil.

We also compare the simulations of albedo (averaged over three grid cells) to observations made by Culf et al. (1996) (Fig. 5a). The seasonality of albedo in the model results is much smaller than observed, although there is a large intersite variability in the observed data. This variability may be a consequence of different tree species present in the sites (Roberts et al. 1990; McWilliam et al. 1996; Sá et al. 1996), and their associated differences in optical properties. However, the variability of canopy radiative properties among different species is very hard to include in the current generation of models.

Because of the strong dependence of seasonal LAI on geographic position, we compare simulated and observed LAI at two sites (Manaus and Ji-Paraná), instead of the basin-wide average. There are currently no direct measurements of seasonal changes in LAI reported in the literature, so we are presenting the results from Roberts et al. (1996), who used the litter method, which is more representative of the annual mean LAI. At the Manaus site, the model shows that the LAI stays nearly constant (at around 6.0) during the entire year. However, at the Ji-Paraná site, the model shows a strong seasonal cycle of LAI. The annual mean LAI reported by Roberts et al. (1996) for this site (LAI = 4.7) is in the range of the simulated LAI annual extremes for the correspondent grid cell.

6. Effects of deforestation

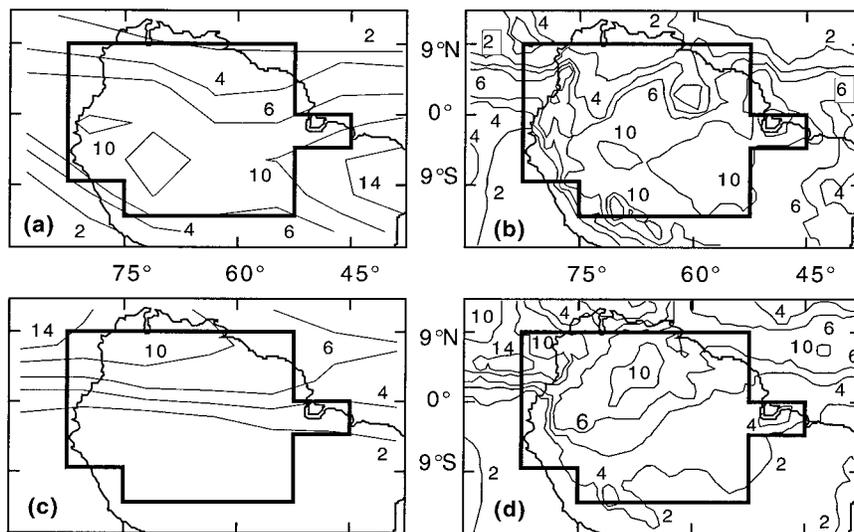In this section, results for the deforested simulation (*D*) are presented. The results are evaluated against

FIG. 4. Spatial patterns of precipitation (mm day^{-1}) for (a) simulated (*F*) values for JFM, (b) observed values for JFM, (c) simulated (*F*) values for JAS, and (d) observed values for JAS. Observed values are from Legates and Willmott (1990).
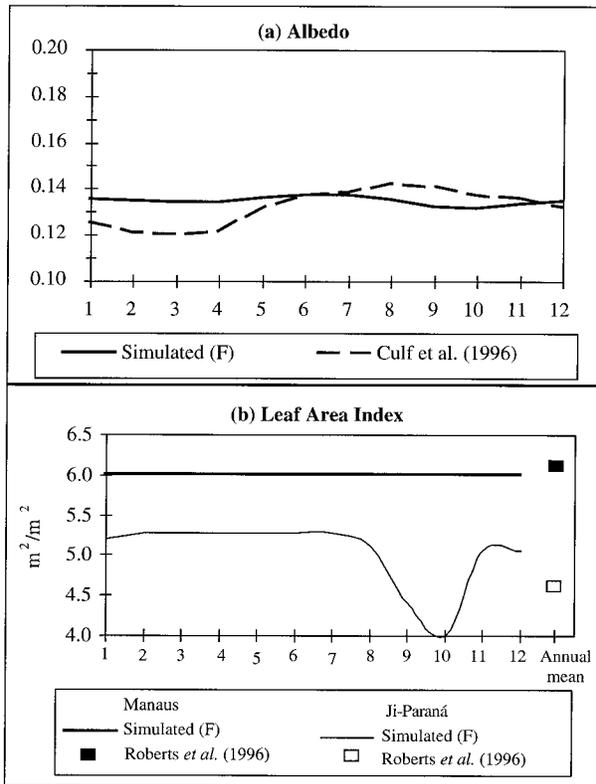
FIG. 5. Seasonal variation of simulated and observed (a) forest α and (b) forest LAI.

FIG. 6. Seasonal variation of simulated and observed (a) pasture LAI and (b) pasture α, in the D simulation.

ABRACOS observations and comparisons are made with other AGCM studies. The differences between this simulation (D) and the control simulation (F) establish the sensitivity of the model to deforestation.

A summary of the annual mean simulation results for the deforested simulation is presented in Tables 1 (climatic response) and 4 (biophysical characteristics). Precipitation decreases after deforestation ($D - F$), consistent with most AGCM experiments. Evapotranspiration also decreases after deforestation, a common result of all tropical deforestation studies (modeling, theoretical, or observational). The decrease in transpiration (53%) is much larger than the decrease in the total evapotranspiration (16%), which indicates that evaporation from the surface partially compensated for the drop in transpiration. Manzi and Planton (1996) and Costa and Foley (1997) found similar results. The response of the model to deforestation might have been greater if the roughness length of the forest (and the change in roughness length) were higher.

The average LAI of the deforested land in this simulation is within the range of published measurements. However, the LAI of grasses is one the most difficult parameters to work in this type of simulation. The LAI of pastures depends on several factors, including 1) the species planted (which is hard to simulate), 2) the seasonal characteristics of the grass (possible to simulate),
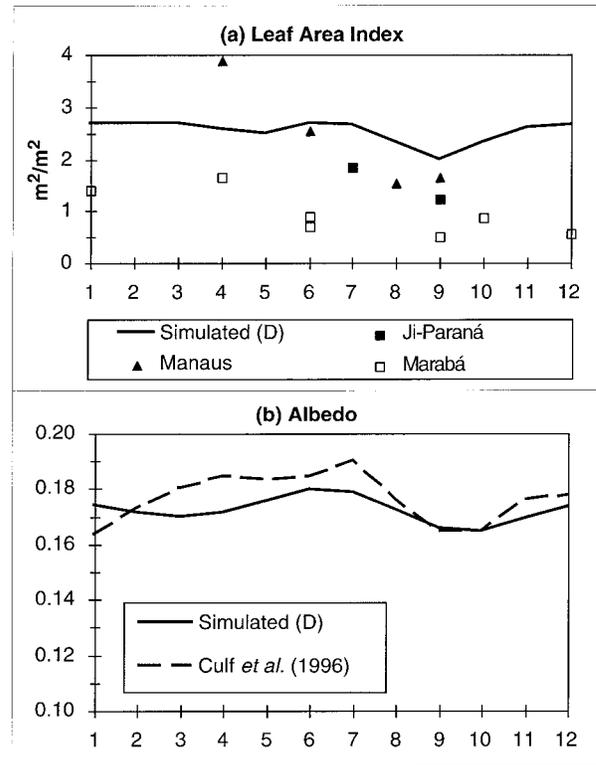
and 3) in real conditions, the consumption of grasses by cattle (currently difficult to simulate). The simulated annual-mean albedo (α) of deforested land matches the average albedos reported by Culf et al. (1996), and the roughness length (z_0) of deforested land is also well simulated by the model (Wright et al. 1996).

Observed seasonal variations in LAI (Fig. 6a, from Roberts et al. 1996) clearly shows that pasture LAI has strong intersite variability. The simulated LAI (Fig. 6a) is calculated using the average of all deforested grid cells and overestimates the observed values. In our interpretation, this happened because we choose a uniform pasture for the whole area, with maximum LAI = 2.7, as recommended by Wright et al. (1996). In future simulations, it will probably be better to allow variations in the pasture LAI from one grid cell to another, to include the effect of species variability among farms and regions.

The seasonal behavior of simulated (D) and observed albedo (Culf et al. 1996) for pasture systems (Fig. 6b) demonstrates that, despite the species variability and the problems with the LAI, the simulated seasonal albedo agrees with the observed, although the simulated seasonality is still smaller than the observed.

Figure 7 shows the seasonal variation of precipitation, evapotranspiration, runoff, and temperature in the F and D experiments. Precipitation is lower in the deforested case in all months except December, but the difference
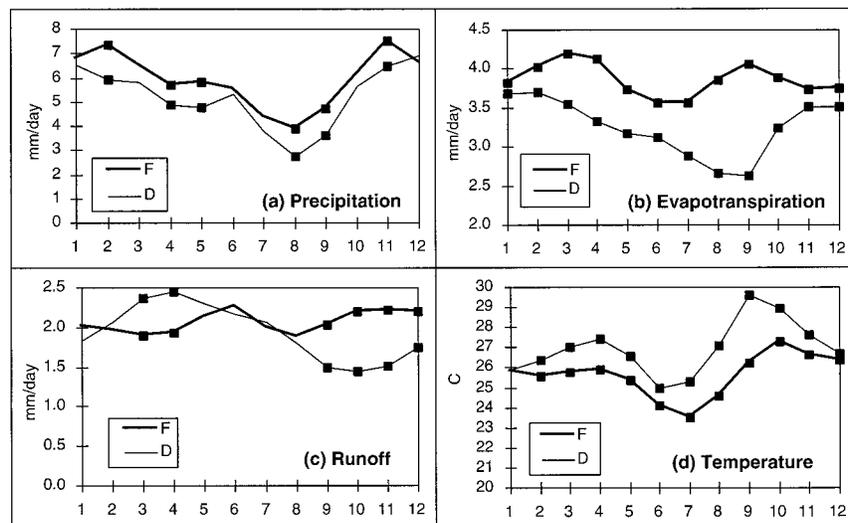
FIG. 7. Seasonal variation of (a) precipitation, (b) evapotranspiration, (c) runoff, and (d) surface temperature in the *F* and *D* experiments. Values marked with a ■ (small square) are different at the 5% significance level, acording to the *t* test.

is statistically significant at the 5% level (according to the *t* test) in only half of the months (Fig. 7a). The seasonality of the precipitation did not change significantly, with the rainy season and dry season occurring in the same periods in both experiments.

The differences in evapotranspiration are statistically significant in all months (Fig. 7b). There are several reasons why pasture evapotranspiration is smaller than in the forest. The main reasons are the changes in albedo and roughness length, which have about the same importance (Lean and Rowntree 1997; Hahmann and Dickinson 1997). Pasture albedo is higher, causing less energy to be absorbed by the surface, while the reduced roughness length in the pasture implies reduced turbulent transfer between the atmosphere and the land surface. However, differences in leaf area and rooting depth also play an important role. Forest evapotranspiration is controlled by the availability of energy; its 12-m root system always supplies water to the trees, even in the dry season. On the other hand, because most pasture roots are above 1.0 m in the soil column, pasture evapotranspiration is also controlled by the soil moisture, and it reaches the maximum during the rainy season and the minimum in the dry season.

Runoff, which is the residual of the balance between

precipitation and evapotranspiration, is one of the hardest parts of the hydrological cycle to simulate in an AGCM. Previous AGCM simulations of deforestation have reported a wide range of changes in runoff after a deforestation, which range from -0.9 to $+0.4$ mm day^{-1} (Table 4). In this study, annual mean runoff is somewhat reduced by deforestation. In addition, there is a strong increase in the seasonality of runoff in the deforested case (Fig. 7c). During the rainy season, *D* runoff is greater than *F* runoff; the inverse happens during the dry season.

On the annual average, the deforestation scenario results in a 1.4°C temperature increase, which is within the range of other published AGCM studies (Table 1). During the seasonal cycle, temperature is significantly higher after deforestation in all months except January (Fig. 7d).

Changes in the hydrologic cycle resulting from deforestation are manifested throughout the basin. Changes in precipitation ($D - F$) for the periods JFM and JAS show considerable differences (Fig. 8), mainly in the northern part of the deforested area. The spatial pattern of the difference ($D - F$) in evapotranspiration is presented in Fig. 9. In JFM, the decrease in the evapotranspiration is small, and the region of maximum decrease is associated with the drop of precipitation in the same area (Fig. 8a). In JAS, evapotranspiration is considerably smaller in *D* than in *F*. This result shows how the pasture is more dependent on the soil moisture than the forest. In the southern part of the basin, which has a dry season of the same intensity in both the *F* and *D* cases (change in the precipitation is small; see Fig. 8b), the evapotranspiration is considerably smaller in the pasture system than in the forest.

TABLE 4. Annual mean of the biophysical characteristics of the pasture and comparisons with other deforestation experiments and ABRACOS results.

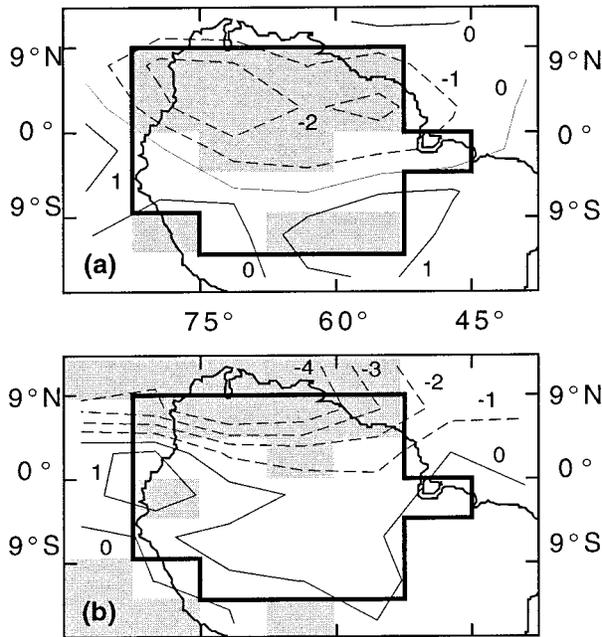|	Simulated (*D*)	Other studies	Source
LAI (m² m⁻²)	2.53	0.5–4.0	Roberts et al. (1996)
α (%)	17.3	17.7	Culf et al. (1996)
z_0 (m)	0.055	0.053	$Z_0 = 0.10\ h_c$, $h_c = 0.53$ m (Wright et al. 1996)

FIG. 8. Spatial patterns of the modeled difference ($D - F$) in precipitation (mm day^{-1}) for (a) JFM and (b) JAS. Shaded regions indicate that the D and F values are different at the 5% significance level, according to the t test.
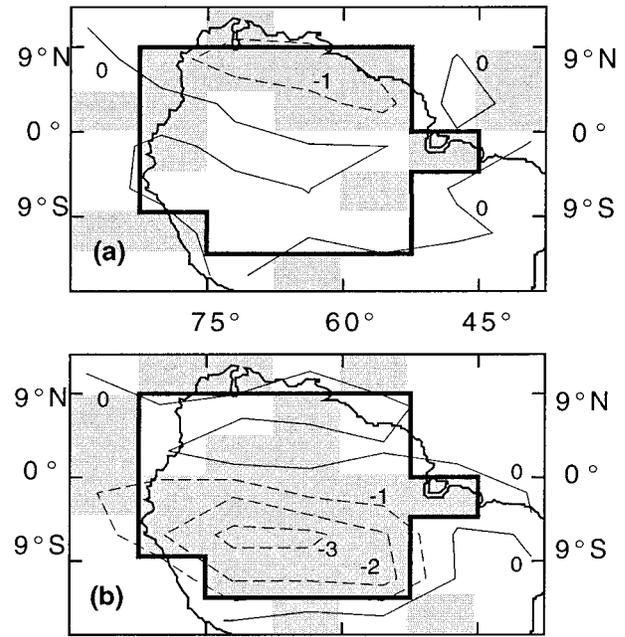

FIG. 9. Spatial patterns of the modeled difference ($D - F$) in evapotranspiration (mm day^{-1}) for (a) JFM and (b) JAS. Shaded regions indicate that the D and F values are different at the 5% significance level, according to the t test.

7. Physiological and radiative effects of CO_2

In this section, results for the $2 \times CO_2$ simulation of the forested scenario (FPR) are presented. The differences between this simulation and the control simulation (F) establish the sensitivity of the model to the physiological and radiative effects of CO_2 on the climate of Amazonia. A discussion about the physiological effects alone (without radiative forcing) can be found in appendix A.

Because very few studies of $2 \times CO_2$ have considered both the physiological and radiative effects of CO_2, one must be very careful when comparing the results of this simulation with other $2 \times CO_2$ experiments. The physiological effects can either enhance or weaken the radiative effect, depending on the variable considered and the region of the world (Sellers et al. 1996a).

The effects of $2 \times CO_2$ on the precipitation are highly uncertain and will depend largely on the AGCM used (see review in section 2). However, the effects on evapotranspiration may be somewhat more conclusive, and they tend to cancel each other: while the physiological effect tends to decrease evapotranspiration through an increase in the water use efficiency of plants, the radiative effect tends to increase evapotranspiration by providing more energy to this process.

In this study, the annual mean evapotranspiration in the FPR experiment exceeds the annual mean evapotranspiration in the control run (F) by 0.14 mm day^{-1} (Table 5). The annual-mean change in evapotranspiration in the FP experiment (see appendix A) is -0.10

mm day^{-1}. Therefore, in Amazonia, the radiative and the physiological effects of CO_2 act in different directions, but the radiative effect is stronger, leading to an overall increase in evapotranspiration.

The physiological and radiative effects of CO_2 both contributed to an overall increase in precipitation over the Amazon basin. In the FPR simulation, the annual mean precipitation increases 0.28 mm day^{-1} (compared to the control run, Table 5), of which only 0.08 mm day^{-1} can be attributed to the physiological effects (appendix A).

The seasonal cycles of precipitation, evapotranspiration, runoff, and temperature for the F and FPR simulations are shown in Fig. 10. The changes in precipitation between the two simulations are not significant during most of year except in April and December. On the other hand, the FPR evapotranspiration is significantly higher than the F evapotranspiration in most months of the year. The most noticeable regional climatic change is an increase in the temperature, as expected from the radiative forcing of CO_2.

Figure 11 presents the spatial pattern of the difference

TABLE 5. Summary of the results for the main experiments.

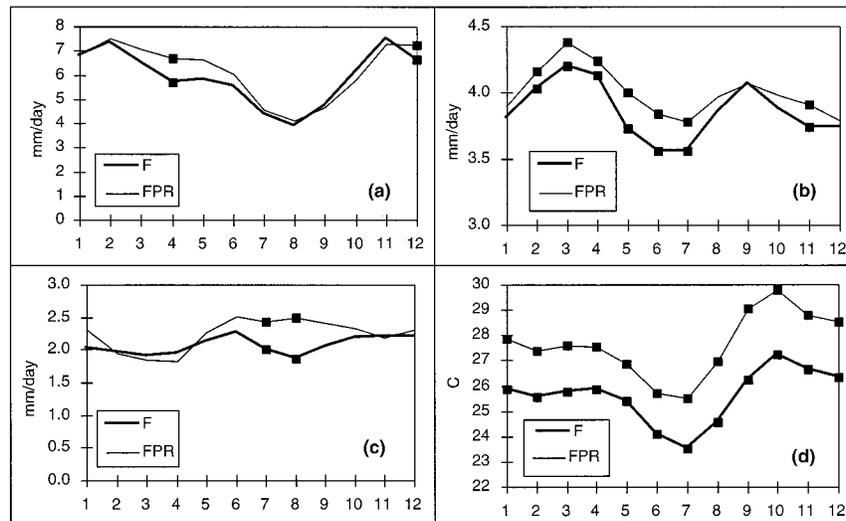|	D	FPR	DPR
ΔP (mm day^{-1})	-0.73	$+0.28$	-0.42
ΔE (mm day^{-1})	-0.61	$+0.14$	-0.40
ΔR (mm day^{-1})	-0.12	$+0.18$	-0.04
ΔT (°C)	$+1.4$	$+2.0$	$+3.5$

FIG. 10. Seasonal variation of (a) *P,* (b) *E,* (c) *R,* and (d) surface temperature in the *F* and FPR experiments. Values marked with a ■ (small square) are different at the 5% significance level, according to the *t* test.

(FPR − *F*) in precipitation resulting from a doubling of CO_2. No significant changes happened in JFM, while there is an increase in the precipitation in the northeast of the area of during JAS. These changes are consistent with the results presented in the 1995 IPCC report (Kattenberg et al. 1996).

The changes in the evapotranspiration resulting from CO_2 effects (Fig. 12) are of much smaller magnitude

than in the deforestation case (Fig. 9). An increase in evapotranspiration is found throughout the region, except in southern Amazonia in JAS (Fig. 12b), which is probably a combined effect of drier soils and lower LAI from leaf senescence.

8. Combined effects of deforestation and CO_2

In this section, results for the combined experiment (DPR), which includes both the effects of deforestation and of $2 \times CO_2$, are presented. As before, both the physiological and radiative effects of CO_2 are explicitly considered. The differences between this simulation and the control simulation (*F*) establish the sensitivity of the model to the combined effects of deforestation plus the physiological and radiative effects of CO_2 on the climate of Amazonia.

a. Surface climate and biophysical characteristics

As seen in sections 6 and 7, deforestation and CO_2 have opposing effects in the two major components of the water balance of the Amazon basin. While deforestation tends to decrease precipitation and evapotranspiration, CO_2 tends to increase these terms. Overall, it appears that the effects of deforestation are the dominant of the two factors. In the combined DPR experiment, the annual mean precipitation decreased by 0.42 mm day^{-1}, while the annual mean evapotranspiration decreased by 0.40 mm day^{-1}. The ΔR is only −0.04 mm day^{-1}.

Figure 13 shows the differences in precipitation, evapotranspiration, runoff, and temperature between the *F* and DPR experiments. The changes in the precipitation are significant only in the transition from the dry
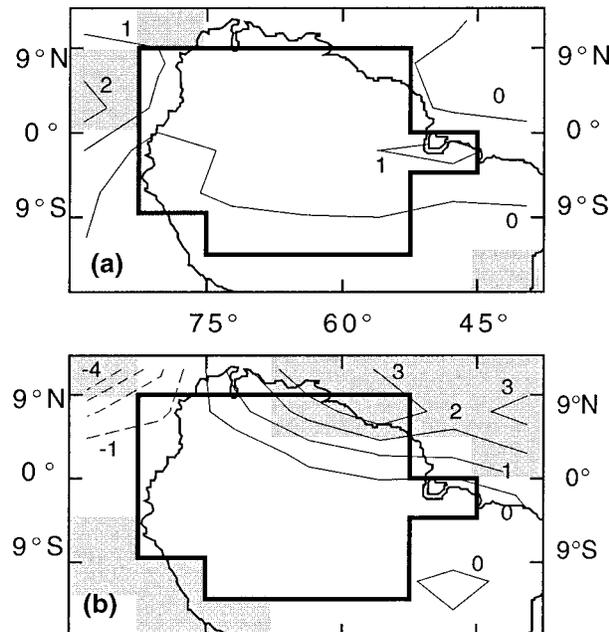

FIG. 11. Spatial patterns of the modeled difference (FPR − *F*) in precipitation (mm day^{-1}) for (a) JFM and (b) JAS. Shaded regions indicate that the FPR and *F* values are different at the 5% significance level, according to the *t* test.
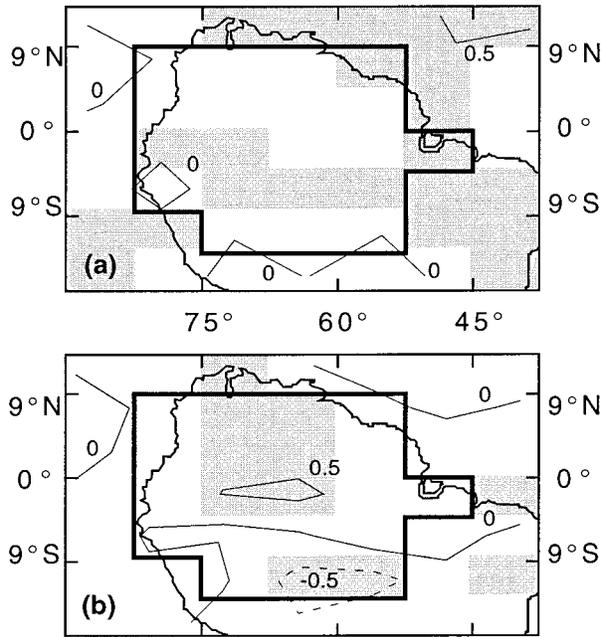
FIG. 12. Spatial patterns of the modeled difference (FPR − F) in evapotranspiration (mm day^{-1}) for (a) JFM and (b) JAS. Shaded regions indicate that the FPR and F values are different at the 5% significance level, according to the t test.

to the rainy season. The DPR evapotranspiration, however, resembles the D behavior (Fig. 7b), which indicates that the D effect dominates over PR. The annual mean change in the runoff is nearly zero, although the amplitude of the DPR curve is higher, again following the D case.

The spatial pattern of precipitation change in DPR −

F (Fig. 14) is basically the same as in $D − F$ (Fig. 8). The decrease in evapotranspiration noted in JFM in northern Amazonia in D (Fig. 9a) is repeated in DPR (Fig. 15a), although attenuated by the effect of the CO_2. In JAS, the PR effect increased evapotranspiration a little in northern Amazonia (Fig. 15b), but in southern Amazonia the deficit of water in the soil dominated and the pattern is similar to $D − F$ (Fig. 9b).

b. Atmospheric circulation

Figure 16 shows the combined effects of deforestation and $2 \times CO_2$ on the atmospheric circulation and the surface temperature, by representing the difference between the experiments DPR and F. Changes in the surface wind (Figs. 16a and 16b) are similar to the sum of the individual effects of deforestation and CO_2. Furthermore, changes in vertical motion at the $\sigma = 0.5$ level in JFM and JAS (Figs. 16c and 16d, respectively) are very similar to the changes produced in the deforestation case (not shown).

Changes in temperature (Figs. 16e and 16f) show the large-scale warming pattern characteristic of a $2 \times CO_2$ scenario. However, the amplitude of the temperature change is substantially enhanced by deforestation: warming is now more than 5°C in northern Amazonia during JFM and more than 9°C in western Amazonia during JAS. Such large increases in temperature (adding to an average temperature that typically exceeds 35°C in JAS) could have profound ecological implications. For example, at such high temperatures, the enzymatic reactions of plants are often severely inhibited, leading to the closure of stomata and a further decrease in evapotranspiration (and an additional increase in canopy temperature). These processes are already represented in
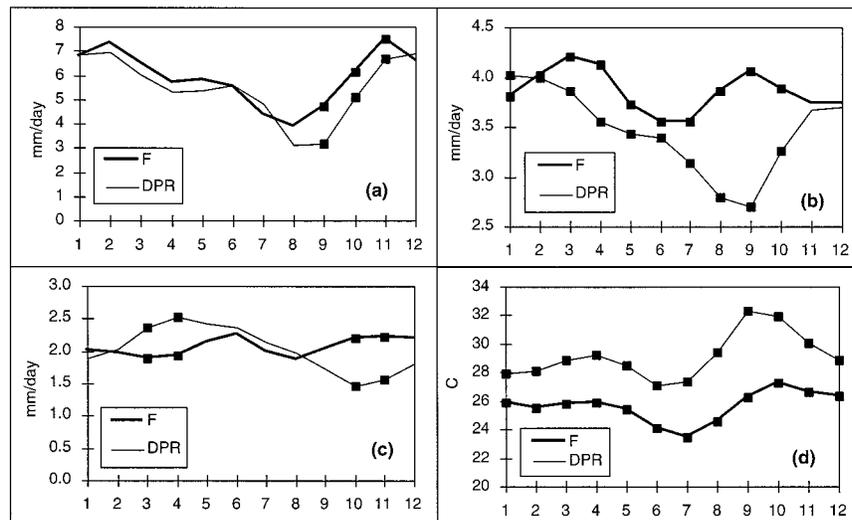

FIG. 13. Seasonal variation of (a) precipitation, (b) evapotranspiration, (c) runoff, and (d) surface temperature in the F and DPR experiments. Values marked with a ■ are different at the 5% significance level, according to the t test.
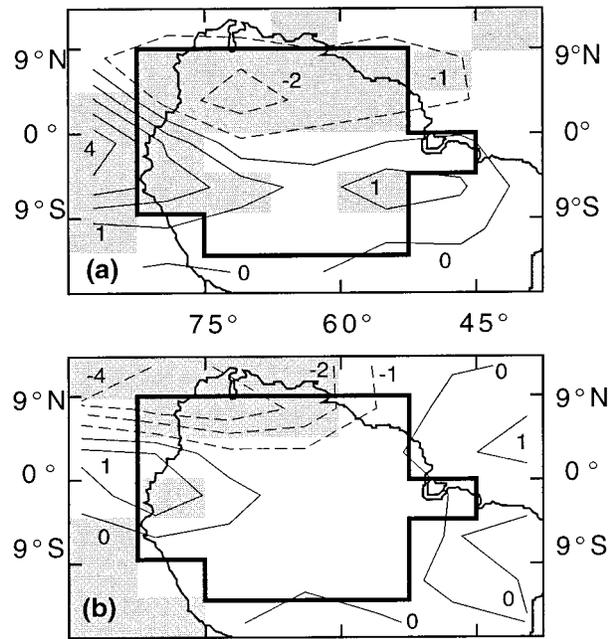
FIG. 14. Spatial patterns of the modeled difference (DPR − F) in precipitation (mm day⁻¹) for (a) JFM and (b) JAS. Shaded regions indicate that the DPR and F values are different at the 5% significance level, according to the t test.

FIG. 15. Spatial patterns of the modeled difference (DPR − F) in evapotranspiration (mm day⁻¹) for (a) JFM and (b) JAS. Shaded regions indicate that the DPR and F values are different at the 5% significance level, according to the t test.
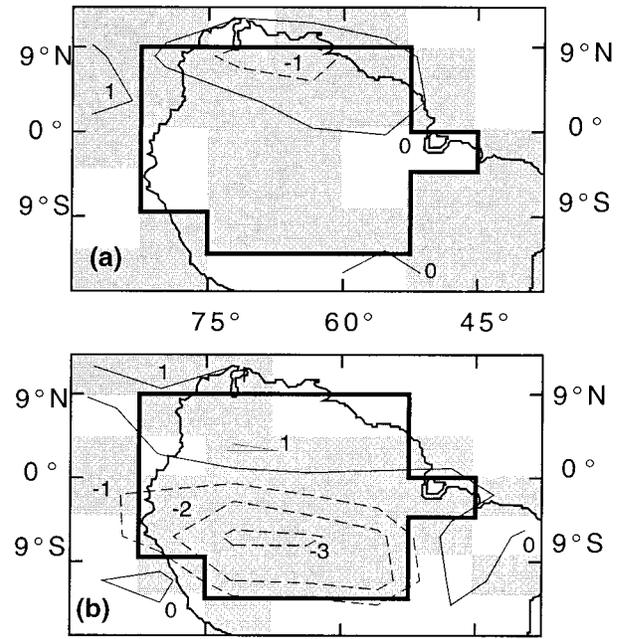
IBIS, so the high temperatures simulated in the DPR experiment already represent this additional effect.

We also analyze the vertically integrated water vapor transport, which is calculated using

$$
\begin{aligned}
Q_\lambda &= \frac{P_1}{g} \int_{\sigma=0}^{\sigma=1} \overline{qu}\, d\sigma \\
Q_\phi &= \frac{P_1}{g} \int_{\sigma=0}^{\sigma=1} \overline{qv}\, d\sigma
\end{aligned} \right\},
\tag{1}
$$

where Q is the vertically integrated transport of vapor, λ refers to the zonal transport, ϕ refers to the meridional transport, P_1 is the pressure at $\sigma = 1$, g is the acceleration due to the gravity, q is the specific humidity, u is the zonal wind, v is the meridional wind, and $\sigma = P/P_1$. The products qu and qv are calculated every time step and accumulated through the month before being vertically integrated.

Transport of water vapor in the DPR experiment (Figs. 16g and 16h) increased significantly along the equatorial region and northern Amazonia, especially in JAS. This caused the annual mean input (output) of water vapor into (out of) Amazonia (as defined in Fig. 2) to increase by 1.21 (1.26) mm day⁻¹, compared to the F experiment.

9. Summary and conclusions

The goal of this study is to examine the sensitivity of the Amazonian climate to the combined effects of deforestation and doubled atmospheric CO_2 concentrations. While it is difficult to construct an accurate scenario of future tropical land use and global atmospheric CO_2 concentrations, it is likely that both will play an increasing role in determining Amazonian climate. Therefore, it is important to consider how these two anthropogenic perturbations to Amazonian climate can interact.

This study illustrates how tropical deforestation and doubled CO_2 concentrations may affect precipitation, evapotranspiration, and temperature in two very different ways (Table 5). For precipitation and evapotranspiration, the effects of deforestation and CO_2 act in opposite directions, weakening each other. For temperature, however, the effects of deforestation and CO_2 enhance each other. Furthermore, it appears that, on the annual mean, the combined effects of tropical deforestation and 2 × CO_2 may be roughly approximated as the linear sum of the individual effects, especially in the cases of the precipitation and temperature (Table 5). In the cases of the evapotranspiration and runoff, the nonlinear term is higher, probably a consequence of the markedly different physiological effect of CO_2 in the rainforest and in the grasses (see Figures A1 and B1).

The combined effects of deforestation and doubled CO_2 concentrations on precipitation, evapotranspiration, and temperature may be considered further.

- *Precipitation.* Deforestation makes the simulated precipitation decrease by 0.73 mm day⁻¹ over the region, which is a consequence of the general decreased ver-
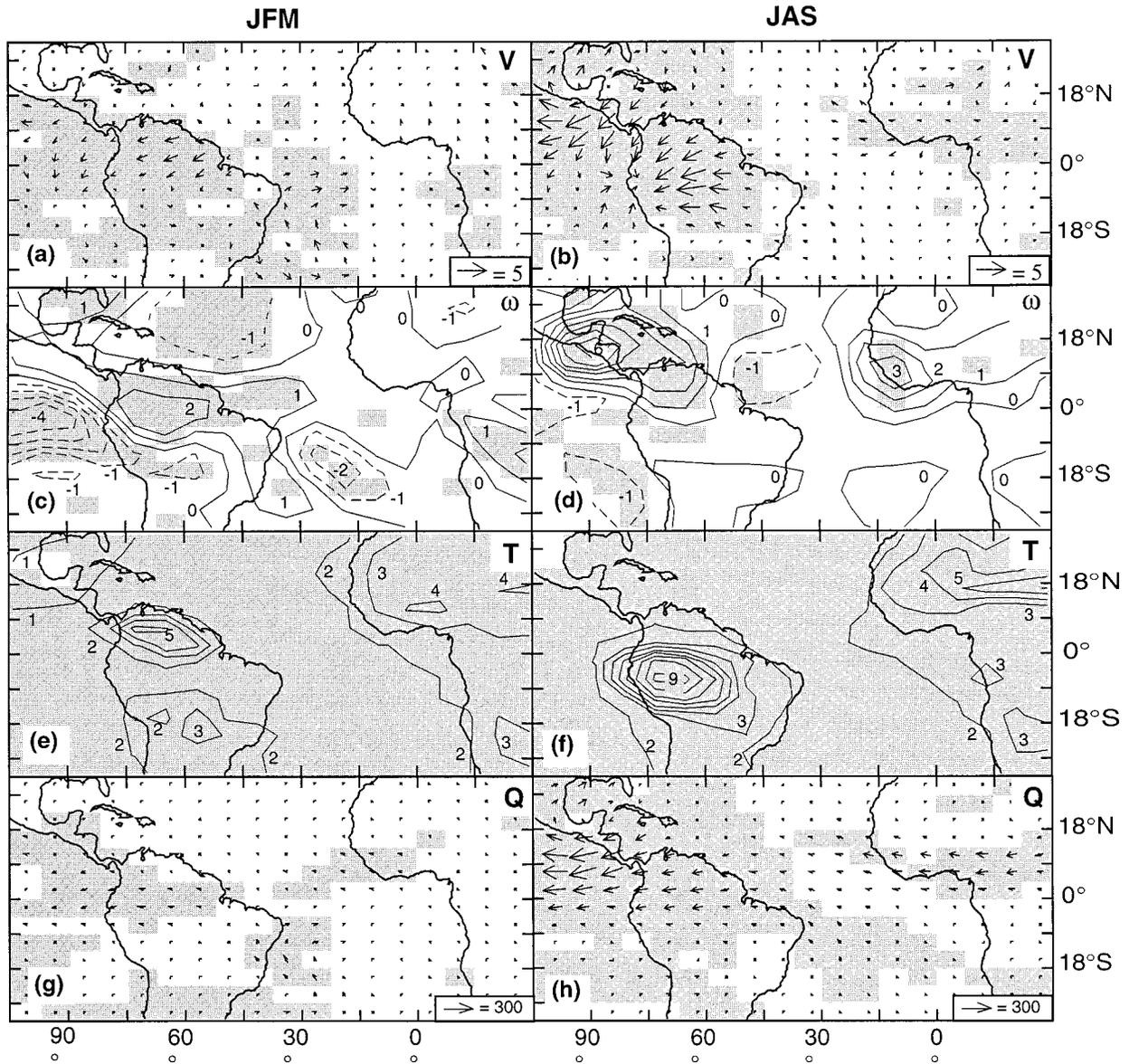
FIG. 16. Spatial patterns of the difference (DPR − F) between some modeled atmospheric circulation and related features. (a) Horizontal wind speed in JFM (m s⁻¹); (b) horizontal wind speed in JAS (m s⁻¹); (c) vertical velocity for JFM, in cPa s⁻¹ (1 cPa = 0.01 Pa); (d) vertical velocity for JAS, in cPa s⁻¹; (e) surface temperature in JFM (°C); (f) surface temperature in JAS (°C). Shaded areas represent the differences that are significant at the 5% level.

tical motion in the atmosphere above the deforested area (although there are some small regions with increased vertical motion). According to Eltahir (1996), the reduction in the net surface radiation after deforestation cools the upper atmosphere over the deforested area, inducing a thermally driven circulation that results in subsidence. CO_2 does not introduce a significant effect on precipitation or the vertical motion, except in the northeastern part of the rainforest area in JAS. The overall effect of CO_2 in Amazonia is an increase in the precipitation of 0.28 mm day⁻¹. The

combined effect of DPR, including the full nonlinear interactions among the processes, is a decrease in the precipitation of 0.42 mm day⁻¹.

• *Evapotranspiration.* Deforestation significantly decreases evapotranspiration through changes in albedo (less energy absorbed), reduced roughness length, shallower roots, and lower leaf area. However, the net effects of $2 \times CO_2$ cause a slight increase in evapotranspiration. The combined effects of deforestation and $2 \times CO_2$ (DPR − F) are a decrease in evapotranspiration of the order of 0.40 mm day⁻¹. In these

TABLE 6. Simulated water balance of the rainforest area. Here R is the runoff; I and O are the advected input and output of water vapor to the region, respectively; C is the convergence of water vapor; and ρ is the precipitation recycling ratio. Units are mm day^{-1}, or %, where noted.

	F	D	FPR	DPR
P	5.92	5.19	6.20	5.50
E	3.86	3.25	4.00	3.46
E/P (%)	65	63	65	63
Tr	2.80	1.30	2.81	1.27
Tr/E (%)	73	40	70	37
R	2.06	1.94	2.24	2.02
I	6.23	6.70	6.87	7.44
O	4.16	4.78	4.70	5.42
C	2.07	1.91	2.17	2.02
ρ (%)	38%	33%	37%	32%

simulations, deforestation decreased runoff, while 2 $\times$ CO$_2$ increased it. The combined effects nearly cancelled each other.

- *Temperature.* Deforestation resulted in increased surface temperature, because of a decrease in evapotranspiration. The physiological effects of CO$_2$ also tend to increase the surface temperature, associated with the decrease in the evapotranspiration. The radiative effect of CO$_2$ is also to increase the surface temperature. The combined effect of DPR, including the interactions among the processes, is an increase in the temperature of the order of 3.5°C.

Most Amazonian deforestation simulations conducted so far [with the exception of Hahmann and Dickinson (1997)] have calculated the moisture convergence to the deforested area using the difference $P - E$, without specifically calculating the water vapor transport in the atmosphere. Table 6 presents a summary of the major components of the simulated water balance of the rainforest area for the four main simulations. Both deforestation and 2 $\times$ CO$_2$ changes caused an increase in the input and output of atmospheric water vapor. Therefore, the DPR experiment (Figs. 16g and 16h) has a large increase of water vapor input and output. There is a small decrease in the net convergence in DPR, which is a balance between the decreased convergence seen in D and increased convergence seen in FPR.

The precipitation–recycling ratio (calculated following Eltahir and Bras 1994) remains nearly constant in both the forested (F and FPR) and deforested (D and DPR) suite of experiments. However, precipitation recycling drops by nearly 5% (absolutely) from the forested (F or FPR) to the deforested (D or DPR) simulations. This result is expected, because of the decreased evapotranspiration rates over pastures. In the end, this means that an Amazonia covered by pasture is more dependent on external sources of water vapor than the same region covered by forest.

While the first simulations of Amazonian deforestation predicted strong changes in regional climate, more recent studies are suggesting that phenomena not considered in these pioneer experiments may act to weaken such climate changes. Some of these processes include the compaction of the subsoil due to the deforestation itself (Lean and Rowntree 1997), water extraction by the deep roots of grasses (Kleidon and Heimann 1999, manuscript submitted to *Climate Dyn.*), and the effects of increasing CO$_2$ concentrations (this study).

However, because deforestation and CO$_2$ tend to change precipitation and evapotranspiration in different directions, the magnitude of each individual effect is decisive in determining the sign of the combined effect. In addition, the climatic response to changes in surface conditions may depend on the AGCM resolution and parameterizations, such as the boundary layer, convective, and cloud parameterizations. Since the magnitude of those effects critically depends on the model used, we recommend that further studies (using different models) should be performed to confirm these results.

APPENDIX A

Physiological Effects of 2 $\times$ CO$_2$ on Forested Conditions (FP $\times$ F)

In this appendix, results for a 2 $\times$ CO$_2$ simulation (FP) on the surface climate are presented. Only physiological effects are considered, and the vegetation cover is the rainforest. A comparison with the control simulation results establishes the sensitivity of the model to the physiological effects of CO$_2$ on the climate of Amazonia in forested conditions.

Figure A1 shows the seasonal variation of precipitation, evapotranspiration, runoff, and surface temperature in the F and FP experiments. No significant changes in the precipitation are found, but there is a significant decrease in the evapotranspiration in all months, except in the period from May to August. Consequently, the runoff increases, but the difference is significant only in April and May. The temperature is a little higher in all months, although the difference is significant only in July and September.

APPENDIX B

Physiological Effects of 2 $\times$ CO$_2$ on Deforested Conditions (DP $\times$ D)

In this appendix, results for a 2 $\times$ CO$_2$ simulation (DP) on the surface climate are presented. Only physiological effects are considered, and the vegetation cover is the pasture. A comparison with the deforested simulation results establishes the sensitivity of the model to the physiological effects of CO$_2$ on the climate of Amazonia in deforested conditions.

Figure B1 shows the seasonal variation of precipitation, evapotranspiration, runoff, and surface temperature in the D and DP experiments. Also in this case,
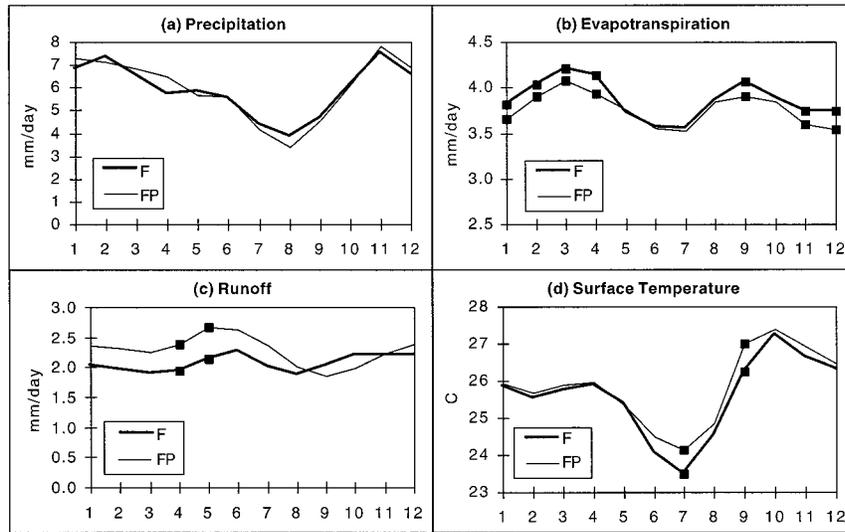
FIG. A1. Seasonal variation of (a) *P,* (b) *E,* (c) *R,* and (d) surface temperature in the *F* and FP experiments. Values marked with a ■ are different at the 5% significance level, according to the *t* test.

there is no significant effect of the change in plant physiology in the precipitation. Similar to the off-line results of Costa and Foley (1997), no significant change in the evapotranspiration is found, except in November. A small increase (not significant) in the evapotranspiration in the beginning of the year may be a consequence of a increase in the precipitation in the same period. The runoff and the surface temperature follow the behavior of precipitation and evapotranspiration.

Comparing the results in appendixes A and B, the conclusion is that the physiological effects of CO_2 are much more important in the rainforest than in grasses.

REFERENCES

Collatz, G. J., J. T. Ball, C. Grivet, and J. A. Berry, 1991: Physiological and environmental regulation of stomatal conductance, photosynthesis and transpiration: A model that includes a laminar boundary layer. *Agric. Forest Meteor.,* **53,** 107–136.
——, M. Ribbas-Carbo, and J. A. Berry, 1992: Coupled photosynthesis-stomatal conductance model for leaves of C_4 plants. *Aust. J. Plant Physiol.,* **19,** 519–538.
Costa, M. H., and J. A. Foley, 1997: The water balance of the Amazon basin: Dependence on vegetation cover and canopy conductance. *J. Geophys. Res. (Atmos.),* **102,** 23 973–23 990.
——, and ——, 1998: A comparison of precipitation datasets for the Amazon basin. *Geophys. Res. Lett.,* **25,** 155–158.
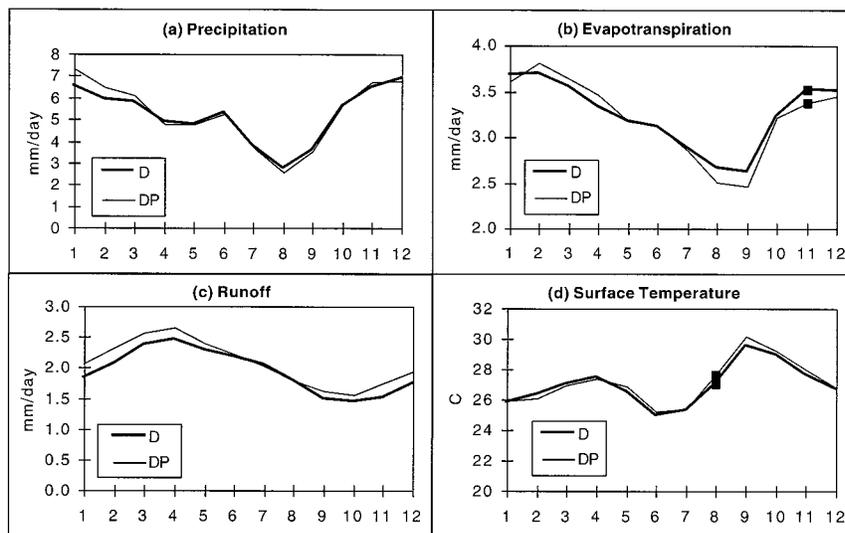
FIG. B1. Seasonal variation of (a) *E,* (b) *P,* (c) *R,* and (d) surface temperature in the *D* and DP experiments. Values marked with a ■ are different at the 5% significance level, according to the *t* test.

Culf, A. D., J. L. Esteves, A. de O. Marques Filho, and H. R. Rocha, 1996: Radiation, temperature and humidity over forest and pasture in Amazonia. *Amazonian Deforestation and Climate,* J. H. C. Gash et al., Eds., John Wiley and Sons, 175–192.

Dickinson, R. E., and P. Kennedy, 1992: Impacts on regional climate of Amazon deforestation. *Geophys. Res. Lett.,* **19,** 1947–1950.

——, A. Henderson-Sellers, P. J. Kennedy, and M. F. Wilson, 1986: Biosphere-Atmosphere Transfer Scheme (BATS) for the NCAR CCM. NCAR/TN-275-STR, National Center for Atmospheric Research, Boulder, CO, 72 pp.

——, ——, and ——, 1993: Biosphere–Atmosphere Transfer Scheme (BATS), version 1e as coupled to the NCAR Community Model. NCAR Tech. Note NCAR/TN-387+STR, National Center for Atmospheric Research, Boulder, CO, 72 pp.

Ducroudé, N., K. Laval, and A. Perrier, 1993: A new set of parameterizations of the hydrologic exchanges at the land–atmosphere interface within the LMD atmospheric general circulation model. *J. Climate,* **6,** 248–273.

Eltahir, E. A. B., 1996: Role of vegetation in sustaining large-scale atmospheric circulations in the tropics. *J. Geophys. Res.,* **101,** 4255–4268.

——, and R. L. Bras, 1994: Precipitation recycling in the Amazon basin. *Quart. J. Roy. Meteor. Soc.,* **120,** 861–880.

Farquhar, G. D., and T. D. Sharkey, 1982: Stomatal conductance and photosynthesis *Ann. Rev. Plant Physiol.,* **33,** 317–345.

——, S. von Caemmerer, and J. A. Berry, 1980: A biogeochemical model of photosynthetic CO_2 assimilation in leaves of C_3 species. *Planta,* **149,** 78–90.

Fearnside, P. M., 1993: Deforestation in Brazilian Amazonia: The effect of population and land tenure. *Ambio,* **22,** 537–545.

Foley, J. A., I. C. Prentice, N. Ramankutty, S. Levis, D. Pollard, S. Sitch, and A. Haxeltine, 1996: An integrated biosphere model of land surface processes, terrestrial carbon balance, and vegetation dynamics. *Global Biogeochem. Cycles,* **10,** 603–628.

Franken, W., and P. R. Leopoldo, 1984: Hydrology of catchment areas of Central-Amazonian forest streams. *The Amazon: Limnology and Landscape Ecology of a Mighty Tropical River and its Basin,* H. Sioli, Ed., Kluwer Academic, 501–519.

Gash, J. H. C., C. A. Nobre, J. M. Roberts, and R. L. Victoria, Eds., 1996: *Amazonian Deforestation and Climate.* John Wiley and Sons, 611 pp.

Hahmann, A. N., and R. E. Dickinson, 1997: RCCM2-BATS model over tropical South America: Applications to tropical deforestation. *J. Climate,* **10,** 1944–1964.

Henderson-Sellers, A., R. E. Dickinson, T. B. Durbidge, P. J. Kennedy, K. McGuffie, and A. J. Pitman, 1993: Tropical deforestation: Modeling local to regional scale climate change. *J. Geophys. Res.,* **98,** 7289–7315.

——, K. McGuffie, and C. Gross, 1995: Sensitivity of global climate model simulations to increased stomatal resistance and CO_2 increases. *J. Climate,* **8,** 1738–1756.

Hodnett, M. G., J. Tomasella, A. de O. Marques Filho, and M. D. Oyama, 1996: Deep soil uptake by forest and pasture in central Amazonia: predictions from long-term daily rainfall data using a simple water balance model. *Amazonian Deforestation and Climate,* J. H. C. Gash et al., Eds., John Wiley and Sons, 79–100.

Houghton, J. T., G. J. Jenkins, and J. J. Ephraums, Eds., 1990: *Climate Change—The IPCC Scientific Assessment.* Cambridge University Press, 365 pp.

Jarvis, P. G., and K. G. McNaughton, 1986: Stomatal control of transpiration: Scaling up from leaf to region. *Adv. Ecol. Res.,* **15,** 1–49.

Kattenberg, A., and Coauthors, 1996: Climate models—Projections of future climate. *Climate Change 1995—The Science of Climate Change,* J. T. Houghton, G. J. Jenkins, and J. J. Ephraums, Eds., Cambridge University Press, 285–357.

Krug, T., 1998: Recent PRODES deforestation estimates. *Second Science Team Meeting of the NASA LBA-Ecology Project,* Hunt Valley, MD, NASA.

Lean, J., and P. R. Rowntree, 1993: A GCM simulation of the impact of Amazonian deforestation on climate using an improved canopy representation. *Quart. J. Roy. Meteor. Soc.,* **119,** 509–530.

——, and ——, 1997: Understanding the sensitivity of a GCM simulation of Amazonian deforestation to the specification of vegetation and soil characteristics. *J. Climate,* **10,** 1216–1235.

Legates, D. R., and C. J. Willmott, 1990: Mean seasonal and spatial variability in gauge-corrected, global precipitation. *Int. J. Climatol.,* **10,** 111–127.

Leopoldo, P. R., W. Franken, E. Matsui, and M. N. G. Ribeiro, 1982: Estimativa da evapotranspiração da floresta amazônica de terra firme. *Acta Amazônica,* **12,** 23–28.

Lesack, L. F. W., 1993: Water balance and hydrologic characteristics of a rain forest catchment in the central Amazon basin. *Water Resour. Res.,* **29,** 759–773.

Leuning, R., 1995: A critical appraisal of a combined stomatal-photosynthesis model for C_3 plants. *Plant, Cell Environ.,* **18,** 339–355.

Manzi, O., and S. Planton, 1996: Calibration of a GCM using ABRACOS and ARME data and simulation of Amazonian deforestation. *Amazonian Deforestation and Climate,* J. H. C. Gash et al., Eds., John Wiley and Sons, 505–530.

McWilliam, A.-L. C., J. M. Roberts, O. M. R. Cabral, M. V. B. R Leitão, A. C. L. da Costa, G. T. Maitelli, and C. A. G. P. Zamparoni, 1993: Leaf area index and above-ground biomass of *terra firme* rainforest. *Funct. Ecol.,* **7,** 310–317.

——, O. M. R. Cabral, B. M. Gomes, J. L. Esteves, and J. M. Roberts, 1996: Forest and pasture leaf-gas exchange in south-west Amazonia. *Amazonian Deforestation and Climate,* J. H. C. Gash et al., Eds., John Wiley and Sons, 505–530.

Mitchell, J. F. B., S. Manabe, V. Meleshko, and T. Tokioka, 1990: Equilibrium climate change—Its implications for the future. *Climate Change—The IPCC Scientific Assessment,* J. T. Houghton, G. J. Jenkins, and J. J. Ephraums, Eds., Cambridge University Press, 131–172.

Monteith, J. L., 1995: Accomodation between transpiring vegetation and the convective boundary layer. *J. Hydrol.,* **166,** 251–263.

Nepstad, D. C., and Coauthors, 1994: The role of deep roots in the hydrological and carbon cycles of Amazonian forests and pastures. *Nature,* **372,** 666–669.

Noilhan, J., and S. Planton, 1989: A simple parameterization of land surface processes for meteorological models. *Mon. Wea. Rev.,* **117,** 536–549.

Page, J. A., 1995: *The Brazilians.* Addison-Wesley, 540 pp.

Polcher, J., and K. Laval, 1994a: The impact of African and Amazonian deforestation on tropical climate. *J. Hydrol.,* **155,** 389–405.

——, and ——, 1994b: A statistical study of regional impact of deforestation on climate in the LMD GCM. *Climate Dyn.,* **10,** 205–219.

Pollard, D., and S. Thompson, 1995: The effect of doubling stomatal resistance in a global climate model. *Global Planet. Change,* **10,** 129–161.

Roberts, J. M., O. M. R. Cabral, and L. F. Aguiar, 1990: Stomatal and boundary-layer conductances measured in a terra firme rain forest, Manaus, Amazonas, Brazil. *J. Appl. Ecol.,* **27,** 336–353.

——, J. P. da Costa, A.-L. C. McWilliam, and T. D. de A. Sá, 1996: An overview of leaf area index and physiological measurements during ABRACOS. *Amazonian Deforestation and Climate,* J. H. C. Gash et al., Eds., John Wiley and Sons, 287–306.

Rocha, H. R., P. J. Sellers, G. J. Collatz, I. R. Wright, and J. Grace, 1996: Calibration and use of the SiB2 model to estimate water vapour and carbon exchange at the ABRACOS forest sites. *Amazonian Deforestation and Climate,* J. H. C. Gash et al., Eds., John Wiley and Sons, 459–472.

Sá, T. D. A., J. P. R. Costa, and J. M. Roberts, 1996: Forest and pasture conductances in southern Pará, Amazonia. *Amazonian Deforestation and Climate,* J. H. C. Gash et al., Eds., John Wiley and Sons, 505–530.

Sellers, P. J., and Coauthors, 1996a: Comparison of radiative and

physiological effects of doubled atmospheric CO_2 on climate. *Science,* **271,** 1402–1406.

——, S. O. Los, C. J. Tucker, C. O. Justice, D. A. Dazlich, G. J. Collatz, and D. A. Randall, 1996b: A revised land surface parameterization (SiB2) for atmospheric GCMs. Part II: The generation of global fields of terrestrial biophysical parameters from satellite data. *J. Climate,* **9,** 706–737.

Shuttleworth, W. J., 1988: Evaporation from Amazonian rainforest. *Proc. Roy. Soc. London B,* **233,** 321–346.

Sud, Y. C., G. K. Walker, J.-H. Kim, G. E. Liston, P. J. Sellers, and W. K.-M. Lau, 1996: Biogeophysical consequences of a tropical deforestation scenario: A GCM simulation study. *J. Climate,* **9,** 3225–3247.

Thompson, S. L., and D. Pollard, 1995a: A global climate model (GENESIS) with a land surface transfer scheme (LSX). Part I: Present climate simulation. *J. Climate,* **8,** 732–761.

——, and ——, 1995b: A global climate model (GENESIS) with a land surface transfer scheme (LSX). Part II: CO_2 sensitivity. *J. Climate,* **8,** 1104–1121.

Warrilow, D. A., A. B. Sangster, and A. Slingo, 1986: Modelling of land surface processes and their influence on European climate. United Kingdom Meteorological Office, Dynamical Climatology Tech. Note DCTN 38, 92 pp. [Available from the United Kingdom Meteorological Office, Bracknell, Berkshire RG12 Z52, United Kingdom.]

Wright, I. R., and Coauthors, 1996: Towards a GCM surface parameterization for Amazonia. *Amazonian Deforestation and Climate,* J. H. C. Gash et al., Eds., John Wiley and Sons, 473–504.

Xue, Y. K., P. J. Sellers, J. L. Kinter III, and J. Shukla, 1991: A simplified biosphere model for global climate studies. *J. Climate,* **4,** 345–364.